

# Charge- and pair-density-wave orders in the one-band Hubbard model from dynamical mean field theory

S. S. Dash<sup>1</sup> and D. Sénéchal<sup>1</sup>

<sup>1</sup>Département de physique and Institut quantique, Université de Sherbrooke, Sherbrooke, Québec, Canada J1K 2R1  
(Dated: March 15, 2022)

We use cluster dynamical mean field theory (CDMFT) on the one-band Hubbard model for the high- $T_c$  superconducting cuprates to study the charge-density-wave phase and its competition with superconductivity at  $T = 0$ . The  $d$ -wave charge-density-wave order, which appears as a  $d$ -wave bond-density-wave order within the one-band Hubbard model, arises purely out of local correlation effects and also leads to a  $s'$ -wave pair-density-wave in the presence of  $d$ -wave superconductivity. The  $d$ -wave bond-density-wave order is observed to be weakened in presence of superconductivity, as has been seen earlier in experiments, and additionally demonstrates strikingly different behaviors on varying  $U$  in the normal and the superconducting states. In the normal state, the  $d$ -wave bond-density-wave order tends to decrease to zero as  $U \rightarrow \infty$  suggesting that it is mediated by magnetic interactions.

## I. INTRODUCTION

Charge-density-wave (CDW) order is ubiquitous among various families of high- $T_c$  superconducting cuprates (HTSC) [1–4]. Although the exact role of this broken-symmetry state in high- $T_c$  superconductivity is not yet understood, it has been observed that the CDW order is in competition with superconductivity [1, 5–7]. It is enhanced when superconductivity is suppressed by a magnetic field.

The CDWs are observed to exist mostly as unidirectional domains [2–4] and are known to have a predominant  $d$ -wave form factor with weak  $s$ -wave and  $s'$ -wave components [3, 8]. CDWs are generally incommensurate [1, 5–7, 9, 10] and the associated wave number decreases with hole doping [5, 10]. However, Kohsaka *et al.* [2] and Fujita *et al.* [3] suggest that a locally commensurate CDW with wavevector  $q = 0.25$  renders the experimental results very well. Further, it was recently observed that a  $s'$ -wave Cooper-pair-density-wave (PDW) order, with wavevector  $q = 0.25$ , exists in underdoped cuprates [11, 12], arising from the coexistence of a  $d$ -wave CDW order and  $d$ -wave superconductivity [11].

There have been many theoretical attempts to study the CDW order as originating from strong correlation effects. For instance, CDW modulations have been obtained from a large- $N$  slave-boson mean-field formulation of the  $t$ - $J$  model [13, 14]. Sachdev & La Placa [15] obtained an incommensurate bond-density-wave order from a Hartree-Fock computation within the  $t$ - $J$  model. Raczkowski *et al.* [16] obtained spatially modulated charge-density and superconductivity using renormalized mean-field theory and variational Monte Carlo on the  $t$ - $J$  model. Pépin *et al.* [17] and Wang & Chubukov [18] obtained the CDW modulations using a spin-fermion model with short-range magnetic interactions. Atkinson *et al.* [19] studied the three-band Hubbard model with a generalized random-phase approximation (RPA) and observed the onset of a CDW order. A recent work using the dynamical cluster approximation (DCA) on the half-filled extended Hubbard model observed the CDW phase [20]. Further, Faye and Sénéchal [21] studied the one-band Hubbard model using the variational clus-

ter approximation (VCA), where they observed the onset of a bond-density-wave order and a pair-density-wave order within the superconducting state.

In this work, we study doped Mott insulators at zero temperature using cluster dynamical mean field theory (CDMFT) with exact diagonalization (ED) as the impurity solver. We observe the existence of various density-wave ( $s$ -,  $s'$ - and  $d$ - wave) orders for a finite range of hole doping, with a dominant  $d$ -wave bond-density-wave (BDW) order. We study the normal and the superconducting states of the system and also observe the appearance of a pair-density-wave (PDW) order when the BDW coexists with superconductivity. Further, we observe that the BDW order is weakened in presence of superconductivity as observed in refs. [6, 7], compared to the BDW order in the normal state. Additionally, the superconducting order is also weakened in presence of the BDW order compared to superconductivity present alone, indicating an inherent competition between the two orders. We also observe that the dependence of the BDW order on  $U$  is very different between the normal and the superconducting states.

The paper is organized as follows. In section II, we briefly describe the one-band Hubbard model and how the density-waves are incorporated within this model. In section III, we describe the CDMFT procedure. In section IV, we show the important results of this work and in section V, we discuss various implications of our results, to finally conclude.

## II. MODEL

We use the one-band Hubbard model:

$$H = - \sum_{\mathbf{r}, \mathbf{r}', \sigma} t_{\mathbf{r}\mathbf{r}'} c_{\mathbf{r}, \sigma}^\dagger c_{\mathbf{r}', \sigma} + U \sum_{\mathbf{r}} n_{\mathbf{r}, \uparrow} n_{\mathbf{r}, \downarrow} - \mu \sum_{\mathbf{r}, \sigma} n_{\mathbf{r}, \sigma} \quad (1)$$

where  $c_{\mathbf{r}, \sigma}^\dagger$  creates an electron of spin  $\sigma$  at the site  $\mathbf{r}$ ;  $U$  is the on-site Coulomb repulsion and  $\mu$  is the chemical potential. We consider only the first, second and third nearest neighbor hopping terms, with amplitudes  $t$ ,  $t'$  and  $t''$  respectively. We adopt the values  $t'/t = -0.3$ ,  $t''/t = 0.2$ ,

appropriate for BSCO [22] and, to some extent, for YBCO [23].

The CDW modulations exist on the oxygen atoms in the  $\text{CuO}_2$  lattice [2, 3]. In the one-band Hubbard model, since oxygen atoms are not explicitly present, the CDWs are best represented as bond-density-wave (BDW) modulations on the Cu-Cu bonds (Fig. 1(a)).

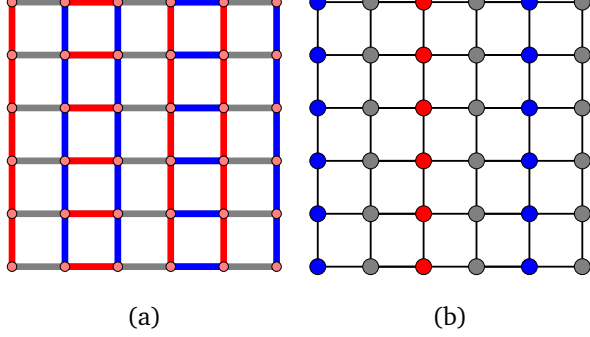


FIG. 1. (a)  $d$ -wave BDW (PDW) modulation on the lattice (red indicates the negative amplitude, blue indicates the positive amplitude and gray indicates zero). An  $s'$ -wave modulation can be visualized by swapping the colors of the bonds (red  $\rightarrow$  blue, blue  $\rightarrow$  red) along any one of the axes. (b)  $s$ -wave CDW modulation on the Cu sites, color code is same as in (a).

The BDW operator can be written as:

$$\hat{\Psi}_{\text{BDW}} = \sum_{\sigma, \mathbf{a}} t_{\mathbf{q}, \mathbf{a}} c_{\mathbf{r}, \sigma}^\dagger c_{\mathbf{r}+\mathbf{a}, \sigma} e^{i\mathbf{q} \cdot (\mathbf{r}+\mathbf{a}/2)} + \text{H.c.} \quad (2)$$

where  $t_{\mathbf{q}, \hat{x}} = -t_{\mathbf{q}, \hat{y}}$  leads to a  $d$ -wave form factor and  $t_{\mathbf{q}, \hat{x}} = t_{\mathbf{q}, \hat{y}}$  leads to a  $s'$ -wave form factor;  $\mathbf{a} = \pm \hat{x}, \pm \hat{y}$ ; since we are looking for modulations on the first-neighbor bonds (Fig. 1(a)) where oxygen atoms should lie.

The  $s$ -wave CDW operator corresponding to the charge-density modulations centered on the Cu sites (Fig. 1(b)) is written as:

$$\hat{\Psi}_{\text{CDW}} = \sum_{\sigma} c_{\mathbf{r}, \sigma}^\dagger c_{\mathbf{r}, \sigma} e^{i\mathbf{q} \cdot \mathbf{r}} + \text{H.c.} \quad (3)$$

We also probe  $d$ -wave superconductivity, with the pairing operator:

$$\hat{\Psi}_{\text{dsc}} = \sum_{\mathbf{r}} (c_{\mathbf{r}, \uparrow} c_{\mathbf{r} \pm \hat{x}, \downarrow} - c_{\mathbf{r}, \downarrow} c_{\mathbf{r} \pm \hat{x}, \uparrow}) - \sum_{\mathbf{r}} (c_{\mathbf{r}, \uparrow} c_{\mathbf{r} \pm \hat{y}, \downarrow} - c_{\mathbf{r}, \downarrow} c_{\mathbf{r} \pm \hat{y}, \uparrow}) + \text{H.c.}, \quad (4)$$

as well as the pair-density-wave (PDW) order with the following operator:

$$\hat{\Psi}_{\text{PDW}} = \sum_{\mathbf{r}, \mathbf{a}} u_{\mathbf{q}, \mathbf{a}} (c_{\mathbf{r}, \uparrow} c_{\mathbf{r}+\mathbf{a}, \downarrow} - c_{\mathbf{r}, \downarrow} c_{\mathbf{r}+\mathbf{a}, \uparrow}) e^{i\mathbf{q} \cdot (\mathbf{r}+\mathbf{a}/2)} + \text{H.c.} \quad (5)$$

where  $u_{\mathbf{q}, \hat{x}} = u_{\mathbf{q}, \hat{y}} = 1$  in a  $s'$ -wave form factor and  $\mathbf{a} = \pm \hat{x}, \pm \hat{y}$ . Motivated by experiments [2, 3], we take  $\mathbf{q} = 2\pi/4\hat{x}$  for all the above DW operators (Eqs 2,3,5).

### III. METHOD

#### A. Cluster Dynamical Mean Field Theory

Short-range quantum fluctuations arising from the strong local Coulomb repulsion are believed to cause the exotic orders mentioned above (Eqs 2-5). Local approaches involving one-electron excitations and formulated in terms of Green functions, such as cluster extensions of dynamical mean field theory, are known to capture these effects well.

In cluster dynamical mean field theory [24], the self-energy of the system is approximated by that of a self-consistent *impurity model*, defined on a small cluster of atoms hybridized with a bath of uncorrelated orbitals. The latter represent the effect of the cluster's environment, i.e., the rest of the lattice. The bath parameters are adjusted self-consistently in such a way that the self-energy of the impurity problem is as close as possible to that of the infinite system. The infinite lattice is tiled into identical, repeated units, i.e., a superlattice of identical clusters is defined, and the cluster coincides with the impurity problem. However, in the present problem, the unit cell of the superlattice is too large to constitute a single impurity problem, and therefore two different impurity problems, each defined on a 4-site plaquette (the cluster), will be necessary to form an 8-site super unit cell (Fig. 2). We use exact diagonalization to solve each impurity model at  $T = 0$ . More information on this approach can be found in [25–27].

Specifically, the impurity model (or cluster) Green function is computed:

$$\mathbf{G}_c(\omega)^{-1} = \omega - \mathbf{t}_c - \Gamma(\omega) - \Sigma(\omega) \quad (6)$$

where  $\mathbf{t}_c$  is the hopping matrix on the cluster,  $\Sigma(\omega)$  is the self-energy of the cluster and  $\Gamma(\omega)$  is the (known) *hybridization function*, which depends on the energies of the uncorrelated orbitals and their hybridization with the cluster, aka the *bath parameters*.

In the case of a single cluster per super unit cell, the lattice Green function can be written as

$$\mathbf{G}(\tilde{\mathbf{k}}, \omega)^{-1} = \omega - \mathbf{t}(\tilde{\mathbf{k}}) - \Sigma(\omega) \quad (7)$$

where  $\Sigma(\omega)$  is the self-energy of the cluster obtained from (6) and is an approximant to the lattice self-energy, and  $\tilde{\mathbf{k}}$  belongs to the Brillouin zone of the superlattice, aka the *reduced Brillouin zone*.  $\mathbf{G}(\tilde{\mathbf{k}}, \omega)$  is a matrix of order  $2L$ ,  $L$  being the number of sites in the super unit cell and the factor of 2 accounting for spin. The CDMFT self-consistency condition states that the local (projected on the cluster) Green function obtained by Fourier transforming the lattice Green function:

$$\bar{\mathbf{G}}(\omega) = \frac{1}{N} \sum_{\tilde{\mathbf{k}}} \mathbf{G}(\tilde{\mathbf{k}}, \omega) \quad (8)$$

should coincide with the cluster Green function  $\mathbf{G}_c(\omega)$ . Because of the finiteness of the bath in the exact diagonalization method, this condition cannot be satisfied exactly and

is instead approximated by the minimization of a distance function

$$d = \sum_{\omega_n} W(z) \text{Tr} \left| \mathbf{G}_c^{-1}(i\omega_n) - \bar{\mathbf{G}}^{-1}(i\omega_n) \right|^2, \quad (9)$$

where the sum is taken over Matsubara frequencies associated with an effective temperature, in order to avoid problems related to the discreteness of the poles in the zero-temperature Green function. When more than one impurity model is needed in the super unit cell, some of the above formulas need to be adapted, as indicated in the next subsection.

### B. Choice of clusters

The size of the super unit cell should be commensurate with the period of the DW modulation we wish to probe, so that the super unit cell contains at least one full DW modulation. In addition, the clusters should be large enough to allow for  $d$ -wave superconductivity to arise from quantum fluctuations within the cluster, and this means 4-site plaquettes.

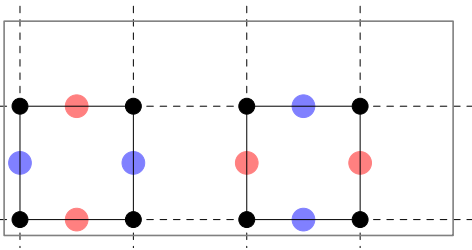


FIG. 2. We choose a  $4a_0 \times 2a_0$  super unit cell (gray box) containing two  $2a_0 \times 2a_0$  clusters. The choice is made so that a full period of the BDW (PDW) modulation (shown in blue and red for positive and negative amplitudes respectively, on the Cu-Cu bonds) lies within the super unit cell. Note that we have shown a  $d$ -wave modulation here; a  $s'$ -wave modulation can be visualized by swapping the colors of the bonds (red  $\rightarrow$  blue, blue  $\rightarrow$  red) along any one of the axes. A  $s$ -wave CDW modulation (Fig. 1(b)) is also contained within our super unit cell.

We therefore define a super unit cell consisting of two  $2 \times 2$  clusters (Fig. 2). Each cluster forms an impurity model with a set of 8 bath orbitals, as specified below. With two clusters in the super unit cell, the lattice Green function takes the form

$$\mathbf{G}(\vec{\mathbf{k}}, \omega)^{-1} = \begin{pmatrix} \omega - \mathbf{t}^{(1)}(\vec{\mathbf{k}}) - \Sigma_1(\omega) & -\mathbf{t}_{ic}(\vec{\mathbf{k}}) \\ -\mathbf{t}_{ic}^\dagger(\vec{\mathbf{k}}) & \omega - \mathbf{t}^{(2)}(\vec{\mathbf{k}}) - \Sigma_2(\omega) \end{pmatrix} \quad (10)$$

where  $\mathbf{t}^{(i)}(\vec{\mathbf{k}})$  is the hopping matrix corresponding to cluster  $i$ ,  $\Sigma_i(\omega)$  is the corresponding self-energy and  $\mathbf{t}_{ic}(\vec{\mathbf{k}})$  is the matrix of hoppings between clusters 1 and 2.

The distance function becomes

$$\sum_{j, \omega_n} W(i\omega_n) \text{Tr} \left| \mathbf{G}_{c,j}^{-1}(i\omega_n) - \bar{\mathbf{G}}_j^{-1}(i\omega_n) \right|^2 \quad (11)$$

where  $j$  is the cluster label.  $\mathbf{G}_{c,j}$  is the  $j^{\text{th}}$  cluster Green function and  $(\bar{\mathbf{G}}^{-1})_j$  is the  $j^{\text{th}}$  diagonal block ( $2N_c \times 2N_c$ ) of the inverse of  $\bar{\mathbf{G}}$  (Eq. (8));  $N_c$  is the number of sites in each cluster.

### C. Bath parametrization

The cluster-bath impurity model is defined by the Hamiltonian

$$H_{\text{imp}} = H_{\text{clus}} + \sum_{\alpha, r, \sigma} \left( \theta_{\alpha, r} c_{\alpha, \sigma}^\dagger a_{r, \sigma} + \text{H.c.} \right) + \sum_{r, \sigma} \epsilon_r a_{r, \sigma}^\dagger a_{r, \sigma} + \sum_{\beta, r} \left[ \Delta_{r, \beta} (c_{\beta \uparrow} a_{r \downarrow} - c_{\beta \downarrow} a_{r \uparrow}) + \text{H.c.} \right] \quad (12)$$

where  $H_{\text{clus}}$  is the restriction of Hamiltonian (1) to the cluster,  $c_{\alpha, \sigma}$  annihilates an electron with spin  $\sigma$  at cluster site  $\alpha$ ,  $a_{r, \sigma}$  annihilates an electron with spin  $\sigma$  in the bath orbital  $r$ ,  $\theta_{\alpha, r}$  is the hopping amplitude from bath orbital  $r$  to site  $\alpha$  on the cluster,  $\epsilon_r$  is the energy of bath orbital  $r$ , and finally  $\Delta_{r, \beta}$  is the pairing amplitude for a singlet formed between site  $\beta$  in the cluster and bath orbital  $r$ . We have put 8 uncorrelated orbitals in the bath; this defines an impurity model of  $2 \times (4 + 8) = 24$  fermionic degrees of freedom (spin included), manageable with an ED solver.

The uncorrelated part of the impurity Hamiltonian (Eq. (12)) can be conveniently represented in matrix form using the Nambu formalism, i.e., in terms of the multiplet  $(C_\uparrow, C_\downarrow, A_\uparrow, A_\downarrow)$ , where  $C_\sigma = (c_{1, \sigma}, c_{2, \sigma}, c_{3, \sigma}, c_{4, \sigma})$  and  $A_\sigma = (a_{1, \sigma}, \dots, a_{8, \sigma})$  ( $\sigma = \uparrow, \downarrow$ ):

$$H_{\text{imp}}^0 = \begin{pmatrix} C_\uparrow^\dagger & C_\downarrow & A_\uparrow^\dagger & A_\downarrow \end{pmatrix} \begin{pmatrix} \mathbf{T} & \Theta \\ \Theta^\dagger & \mathbf{E} \end{pmatrix} \begin{pmatrix} C_\uparrow \\ C_\downarrow \\ A_\uparrow \\ A_\downarrow \end{pmatrix} \quad (13)$$

where

$$\mathbf{T} = \begin{pmatrix} \mathbf{t}_c & \mathbf{0} \\ \mathbf{0} & -\mathbf{t}_c \end{pmatrix}, \quad \Theta = \begin{pmatrix} \boldsymbol{\theta} & -\Delta^\dagger \\ -\Delta^T & -\boldsymbol{\theta}^* \end{pmatrix}, \quad \mathbf{E} = \begin{pmatrix} \boldsymbol{\epsilon} & \mathbf{0} \\ \mathbf{0} & -\boldsymbol{\epsilon} \end{pmatrix} \quad (14)$$

$\mathbf{t}_c$  is a  $4 \times 4$  matrix,  $\boldsymbol{\theta}$  is a  $4 \times 8$  matrix,  $\Delta$  is a  $8 \times 4$  matrix,  $\boldsymbol{\epsilon}$  is a  $8 \times 8$  diagonal matrix with energies of the 8 bath orbitals as the diagonal elements.

The uncorrelated cluster Green function can be obtained by projecting the uncorrelated impurity Green function  $\mathbf{G}_{\text{imp}}^0 = (\omega - H_{\text{imp}}^0)^{-1}$  on the cluster, from which the bath hybridization function  $\Gamma$  in Eq. (6) can be obtained as:

$$\Gamma = \Theta (\omega - \mathbf{E})^{-1} \Theta^\dagger \quad (15)$$

There are 64 parameters in the cluster-bath hybridization  $\Theta$  for each cluster, therefore a total of 128 parameters, w.r.t which the distance function (eq. (11)) should be minimized at each CDMFT iteration. Symmetries of the cluster can help to reduce the number of independent variational parameters. Point group symmetries have been used

to parametrize the bath in CDMFT [28, 29]. We follow Foley *et al.* [29] and parametrize the bath corresponding to the irreducible representations of the point group  $C_2$  generated by a reflexion across the horizontal axis (Fig. 3). The orders that we probe, i.e., the DW and the superconducting orders, are compatible with this point group symmetry.

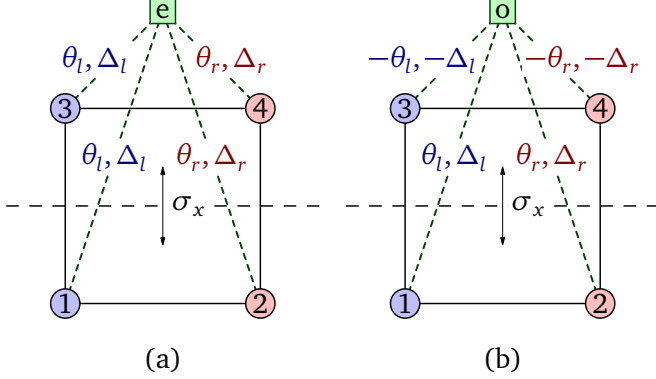


FIG. 3. The cluster-bath hybridization terms ( $\theta$ 's and  $\Delta$ 's in Eq. (12)) are chosen to correspond to the even and odd representations of the  $C_2$  symmetry group, which operates on the cluster sites; (a) shows a cluster-bath hybridization which is even under  $\sigma_x$  and (b) shows a cluster-bath hybridization which is odd under  $\sigma_x$ , corresponding to the two irreducible representations of  $C_2$ .

Figure 3 shows the parametrization of the bath, which contains the even and odd irreducible representations of the symmetry group  $C_2$ . The number of independent parameters in  $\Theta$  is now reduced to 32 per cluster. Out of 8 bath orbitals, 4 belong to the even irreducible representation (Fig. 3(a)) and 4 belong to the odd irreducible representation (Fig. 3(b)). The matrices  $\theta$  and  $\Delta$  take the following form for the even (Eqs (16-17)) and odd (Eqs (18-19)) irreducible representations:

$$\theta_{\text{even}} = \begin{pmatrix} \theta_{l1} & \theta_{l2} & \theta_{l3} & \cdots & \theta_{l8} \\ \theta_{r1} & \theta_{r2} & \theta_{r3} & \cdots & \theta_{r8} \\ \theta_{l1} & \theta_{l2} & \theta_{l3} & \cdots & \theta_{l8} \\ \theta_{r1} & \theta_{r2} & \theta_{r3} & \cdots & \theta_{r8} \end{pmatrix} \quad (16)$$

$$\Delta_{\text{even}} = \begin{pmatrix} \Delta_{l1} & \Delta_{l2} & \Delta_{l3} & \cdots & \Delta_{l8} \\ \Delta_{r1} & \Delta_{r2} & \Delta_{r3} & \cdots & \Delta_{r8} \\ \Delta_{l1} & \Delta_{l2} & \Delta_{l3} & \cdots & \Delta_{l8} \\ \Delta_{r1} & \Delta_{r2} & \Delta_{r3} & \cdots & \Delta_{r8} \end{pmatrix} \quad (17)$$

$$\theta_{\text{odd}} = \begin{pmatrix} \theta_{l1} & \theta_{l2} & \theta_{l3} & \cdots & \theta_{l8} \\ \theta_{r1} & \theta_{r2} & \theta_{r3} & \cdots & \theta_{r8} \\ -\theta_{l1} & -\theta_{l2} & -\theta_{l3} & \cdots & -\theta_{l8} \\ -\theta_{r1} & -\theta_{r2} & -\theta_{r3} & \cdots & -\theta_{r8} \end{pmatrix} \quad (18)$$

$$\Delta_{\text{odd}} = \begin{pmatrix} \Delta_{l1} & \Delta_{l2} & \Delta_{l3} & \cdots & \Delta_{l8} \\ \Delta_{r1} & \Delta_{r2} & \Delta_{r3} & \cdots & \Delta_{r8} \\ -\Delta_{l1} & -\Delta_{l2} & -\Delta_{l3} & \cdots & -\Delta_{l8} \\ -\Delta_{r1} & -\Delta_{r2} & -\Delta_{r3} & \cdots & -\Delta_{r8} \end{pmatrix} \quad (19)$$

#### D. Computing averages

After the CDMFT procedure has converged, the lattice Green function (10) can be used to compute various observables. The average value of a one-body operator  $\hat{O} = \sum_{\mathbf{r}, \mathbf{r}', \sigma} O_{\mathbf{r}\mathbf{r}'} c_{\mathbf{r}\sigma}^\dagger c_{\mathbf{r}'\sigma}$  is computed as

$$\langle \hat{O} \rangle = \oint \frac{d\omega}{2\pi} \int \frac{d^2\mathbf{k}}{(2\pi)^2} \text{tr}[\mathbf{O}(\tilde{\mathbf{k}})\mathbf{G}(\tilde{\mathbf{k}}, \omega)] \quad (20)$$

, called the lattice average of  $\hat{O}$ . This is the formalism used to measure the order parameters corresponding to the operators (2-5) in this work. Another way of computing the averages of one-body operators is to use the cluster Green function (6), which gives the cluster averages of operators:

$$\langle \hat{O} \rangle_c = \oint \frac{d\omega}{2\pi} \text{tr}[\mathbf{O}\mathbf{G}_c(\omega)] \quad (21)$$

However, the DW operators are not defined fully on each cluster because they are period-4 objects, hence their cluster averages would be meaningless. But for local operators like the density operator, it could be more relevant in some cases to look at the cluster averages than the lattice averages. It is known that CDMFT intrinsically breaks the translation symmetry of the lattice, and this leads to a spurious DW with a period equal to the size of the cluster [30]. We observe such a DW with a period of 2 unit cells in the  $\hat{x}$  direction, but this spurious effect is very different from the period-4 DW defined in (2,3,5), which is accompanied by a difference in the electron densities between the two clusters.

## IV. RESULTS

We have carried out CDMFT computations in three ways: (1) By probing the DW orders and suppressing superconductivity (the normal phase); (2) by probing superconductivity and suppressing the DW orders, which is done by requiring that the two clusters forming the super unit cell have identical bath parameters (the pure SC phase); (3) by allowing all orders (DW and SC) to coexist (the coexistence phase). Note that the coexistence is microscopic in the context of this work.

Figure 4 shows the  $d$ -wave BDW order parameter and other related ( $s'$ - and  $s$ -wave) DW order parameters, as a function of hole doping for different values of the on-site Coulomb repulsion  $U$ , in the normal phase. As can be seen from the figure, the  $d$ -wave BDW is the predominant order, with weaker  $s'$ -wave BDW and  $s$ -wave CDW orders, as also seen in experiments [3, 8]. We will focus on the  $d$ -wave BDW order for the rest of this article. The  $d$ -wave BDW order parameter decreases with  $U$  for most values of hole doping shown. However, as can be seen in Figs 4b and 4c, the relative strengths of the  $s'$ -wave BDW and the  $s$ -wave CDW orders increase with  $U$ .

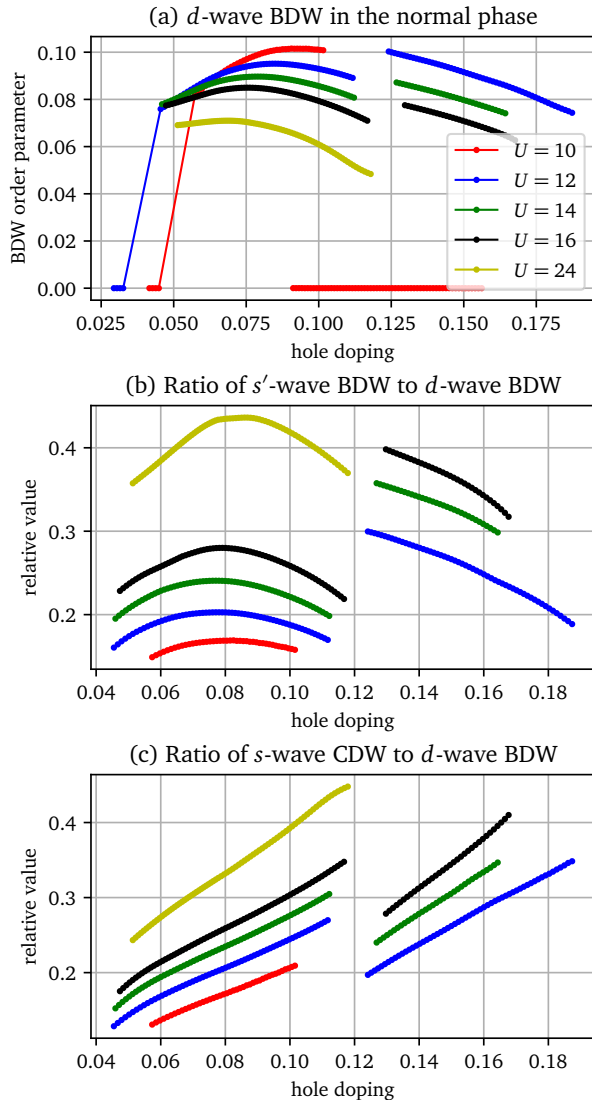


FIG. 4. (a) The  $d$ -wave BDW order parameter as a function of doping for different values of  $U$  in the normal phase. (b) The  $s'$ -wave BDW and (c) the  $s$ -wave CDW order parameters, relative to the  $d$ -wave BDW order.

Figure 5 shows the  $d$ -wave BDW order parameter (filled symbols) in the coexistence phase, where it is also accompanied by a  $s'$ -wave PDW order (open symbols), as recently observed experimentally [11, 12]. It is known from Ginzburg-Landau theory [31, 32] that coexisting  $d$ -wave BDW and  $d$ -wave superconductivity lead to a  $s'$ -wave PDW. Note that the PDW order is much weaker than the BDW order.

It is known that the  $d$ -wave CDW order in cuprates is weakened within the superconducting state [6, 7]. As discussed in Sect. II, such a CDW is incorporated as a  $d$ -wave BDW here. Figure 6 shows the  $d$ -wave BDW order (in red) in the normal phase (open symbols) as well as within the coexistence phase (filled symbols) for  $U = 14$  (Fig. 6a) and  $U = 16$  (Fig. 6b). It can be seen that the BDW order is much weaker in the coexistence phase than in the normal phase.

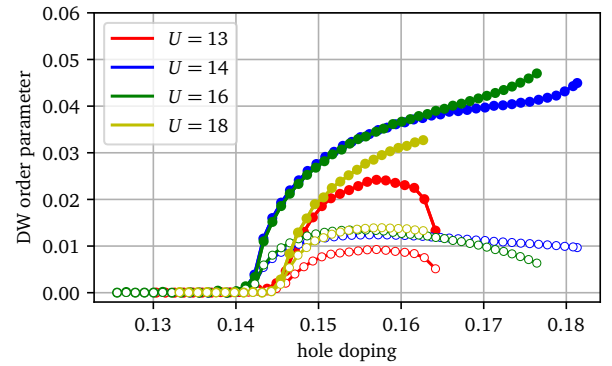


FIG. 5. BDW (filled symbols) and  $PDW \times 10$  (open symbols) order parameters in the coexistence phase for different values of  $U$ .

Fig. 6 also compares the superconducting order parameter (in blue) in the pure SC phase (open symbols) with that in the coexistence phase (filled symbols), and they are seen to coincide when the BDW order goes to zero. Superconductivity is also weakened when it coexists with the BDW order, as can be seen in the figure. Further, the PDW order (in green) is seen to exist only when both BDW and superconductivity are present.

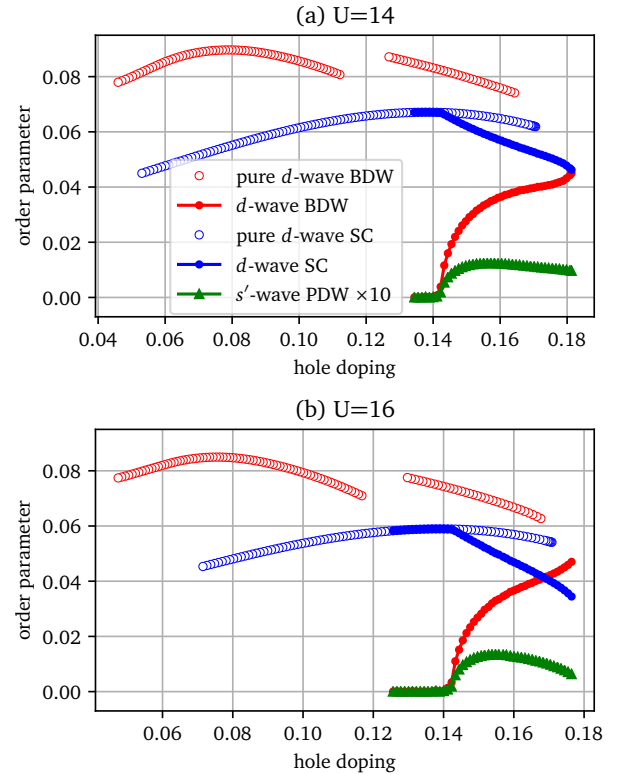


FIG. 6. (a) BDW order parameter (red) in the normal (open symbols) and coexistence (filled symbols) phases along with the superconducting order parameter (blue) in the pure SC (open symbols) and coexistence (filled symbols) phases, for  $U = 14$ . The PDW order (green) is also shown. (b) Same for  $U = 16$ .

Figure 7 shows the  $d$ -wave BDW order parameter (filled

symbols) and the  $d$ -wave superconducting order parameter (open symbols) in the coexistence phase as a function of doping for different values of  $U$ . The BDW order parameter grows from  $U = 13$  to  $U = 14$ , remains almost constant up to  $U = 16$  and then decreases. By contrast, the  $d$ -wave BDW order parameter in the normal state (Fig. 4a) decreases with  $U$ . Such a difference in the behavior of the BDW order as function of  $U$  in the normal and the coexistence phase emphasizes the competition between superconductivity and BDW. Note that superconductivity is weakened upon increasing  $U$ .

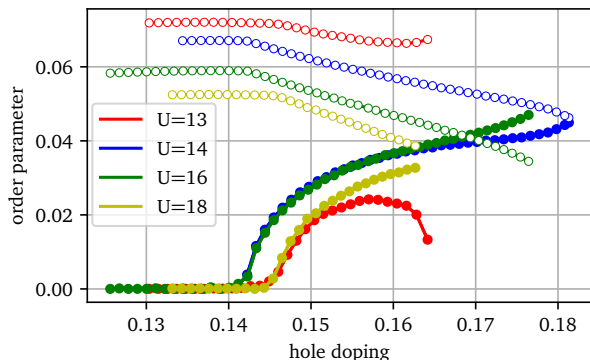


FIG. 7.  $d$ -wave BDW (filled symbols) and superconducting (open symbols) order parameters are shown together for  $U = 13, 14, 16, 18$  in the coexistence phase to emphasize their behaviour as a function of  $U$ .

The period-4 DW orders appear spontaneously in our CDMFT solutions as we reach appropriate doping values. This is marked by a spontaneous breaking of the translation symmetry in our impurity models, i.e., across the two impurity clusters, which constitute the unit cell of the superlattice. For instance, the appearance of the DW orders is accompanied by a difference in the densities between the two clusters. Figure 8 shows the electron densities on the two clusters (red symbols) along with the various DW order parameters (blue symbols) as a function of the lattice doping. This difference in the densities between the two clusters can be attributed to the  $s'$ -wave BDW and the  $s$ -wave CDW orders, which appear along with the dominant  $d$ -wave BDW order as also seen earlier in Fig. 4, since the  $d$ -wave BDW order does not produce a bias in the cluster densities. Further, this is an effect of a period-4 modulation as opposed to a period-2 modulation where the two clusters must be identical.

## V. DISCUSSION AND CONCLUSION

It is usually assumed that  $d$ -wave CDW modulations are mediated by short-range antiferromagnetic (AFM) fluctuations [14, 15, 18]. Various theoretical studies using the  $t$ - $J$  model, a large- $U$  limit of the Hubbard model emphasizing exchange interactions, have been able to compute the CDW modulations in various approximations [13–16]. In our case, the short-range correlations within the 4-site clus-

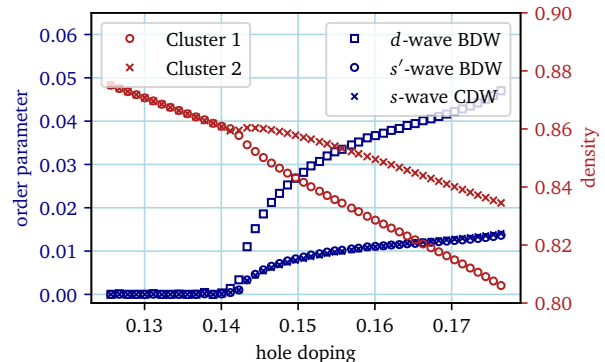


FIG. 8. Cluster densities (red) are shown along with the DW order parameters (blue) for the coexistence phase for  $U = 16$ . The two clusters are identical in the absence of a period-4 DW order, which then start to diverge on their densities as the DW orders develop.

ters govern the physics of the DW modulations. A general effective theory of magnetic interactions at large  $U$  would include ring-exchange and higher order terms in addition to exchange terms and would be formulated as a power series in  $1/U$  [33]. Hence the  $d$ -wave BDW order parameter should decrease with  $U$ , at least when  $U$  is large, and go to zero as  $U \rightarrow \infty$  if it is mediated by AFM fluctuations. In other words, it should not have a component that is  $U$ -independent as  $U \rightarrow \infty$ . We show in Fig. 9 the optimal value of the  $d$ -wave BDW order parameter in the normal phase as a function of  $1/U$ . We also include fits of the data-points against polynomials in  $1/U$  of degrees 1 to 4; the fit coefficients are shown in Table I. The key observation is that the constant term  $a_0$  decreases with the order of the polynomial, which indicates that the optimal order parameter goes to zero as  $U \rightarrow \infty$ . This reinforces our belief that the  $d$ -wave BDW order is mediated by short-range AFM fluctuations.

In the coexistence phase, the behavior of the  $d$ -wave BDW order is not monotonous with  $U$  (Figs 5,7). We observe that both superconductivity and  $d$ -wave BDW order are weakened when coexisting (Fig. 6), suggesting a competition between the two orders [1, 5–7]. This is likely the reason for the difference in the behavior of the BDW order when varying  $U$  between the normal and coexistence phases. Previous studies of hole-doped cuprates have shown that the superconducting  $T_c$  roughly scales as  $J$  [34, 35], which suggests that superconductivity is mediated by magnetic fluctuations and drops at large  $U$ . We observe in Figs 5,7 that the BDW order parameter first increases with  $U$ , concurrently with a drop in superconductivity, and then starts decreasing with  $U$  (like in the normal phase shown in Fig. 4) after its competitor (superconductivity) has been sufficiently weakened. This is another sign of the competition between the two phases, as opposed to cooperation.

The range of hole doping at which BDW occurs in the normal phase is also different than that at which the BDW occurs in the coexistence phase. In the normal phase, the  $d$ -wave BDW order starts at very low hole doping (around

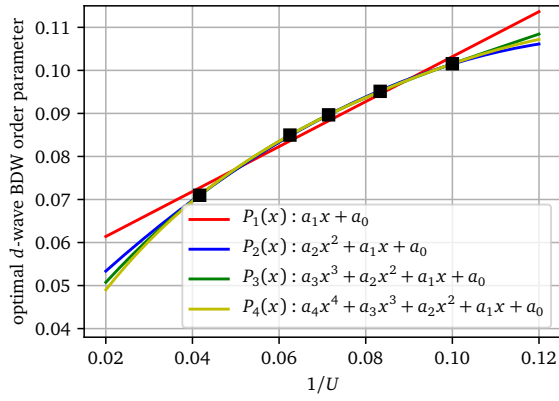


FIG. 9. Optimal value of the  $d$ -wave BDW order parameter in the normal state (Fig. 4(a)) as a function of  $1/U$  along with fits with various polynomial functions. The values of the coefficients for each polynomial function is shown in table I.

TABLE I. Fit parameters of the polynomial functions used in Fig. 9.

	$P_1(x)$	$P_2(x)$	$P_3(x)$	$P_4(x)$
$a_0$	$0.051 \pm 0.0031$	$0.034 \pm 0.0012$	$0.025 \pm 0.00077$	$0.017$
$a_1$	$0.52 \pm 0.042$	$1.043 \pm 0.034$	$1.45 \pm 0.036$	$1.94$
$a_2$		$-3.68 \pm 0.24$	$-9.71 \pm 0.54$	$-20.73$
$a_3$			$28.35 \pm 2.52$	$133.67$
$a_4$				$-366.26$

4%), while in the coexistence phase, it starts at around 14% doping. This disappearance of the BDW order at lower values of the hole doping in the coexistence phase might also be related to the competition between the two orders.

In summary, we obtain various DW orders, dominated by a  $d$ -wave BDW, arising from local correlation effects in the one-band Hubbard model. We observe that both BDW order and superconductivity are weakened when they coexist, revealing the competition between these orders. We also observe a  $s'$ -wave PDW when BDW and superconductivity coexist. Furthermore, the  $d$ -wave BDW order is observed to vanish as  $U \rightarrow \infty$ , which strongly suggests a spin fluctuation mechanism.

#### ACKNOWLEDGMENTS

Fruitful discussions with A. Foley, S. Verret and A.-M. Tremblay are gratefully acknowledged. Computational resources for this work were provided by Compute Canada and Calcul Québec. This work has been supported by the Natural Sciences and Engineering Research Council of Canada (NSERC) under grants RGPIN-2015-05598 and RGPIN-2020-05060.

- [1] G Ghiringhelli, M Le Tacon, Matteo Minola, S Blanco-Canosa, Claudio Mazzoli, NB Brookes, GM De Luca, A Frano, DG Hawthorn, F He, *et al.*, “Long-range incommensurate charge fluctuations in  $(Y,Nd)Ba_2Cu_3O_{6+x}$ ,” *Science* **337**, 821–825 (2012).
- [2] Y Kohsaka, C Taylor, K Fujita, A Schmidt, C Lupien, T Hanaguri, M Azuma, M Takano, H Eisaki, H Takagi, *et al.*, “An intrinsic bond-centered electronic glass with unidirectional domains in underdoped cuprates,” *Science* **315**, 1380–1385 (2007).
- [3] Kazuhiro Fujita, Mohammad H Hamidian, Stephen D Edkins, Chung Koo Kim, Yuhki Kohsaka, Masaki Azuma, Mikio Takano, Hidenori Takagi, Hiroshi Eisaki, Shin-ichi Uchida, *et al.*, “Direct phase-sensitive identification of a  $d$ -form factor density wave in underdoped cuprates,” *Proceedings of the National Academy of Sciences* **111**, E3026–E3032 (2014).
- [4] Riccardo Comin and Andrea Damascelli, “Resonant x-ray scattering studies of charge order in cuprates,” *Annual Review of Condensed Matter Physics* **7**, 369–405 (2016).
- [5] Markus Huecker, Niels Bech Christensen, AT Holmes, Elizabeth Blackburn, Edward M Forgan, Ruixing Liang, DA Bonn, WN Hardy, Olof Gutowski, M v Zimmermann, *et al.*, “Competing charge, spin, and superconducting orders in underdoped  $YBa_2Cu_3O_y$ ,” *Physical Review B* **90**, 054514 (2014).
- [6] J Chang, E Blackburn, AT Holmes, Niels B Christensen, Jacob Larsen, J Mesot, Ruixing Liang, DA Bonn, WN Hardy, A Watenphul, *et al.*, “Direct observation of competition between superconductivity and charge density wave order in  $YBa_2Cu_3O_{6.67}$ ,” *Nature Physics* **8**, 871–876 (2012).
- [7] TP Croft, Christopher Lester, MS Senn, Alessandro Bombardi, and SM Hayden, “Charge density wave fluctuations in  $La_{2-x}Sr_xCuO_4$  and their competition with superconductivity,” *Physical Review B* **89**, 224513 (2014).
- [8] R Comin, R Sutarto, F He, EH da Silva Neto, L Chauviere, A Frano, R Liang, WN Hardy, DA Bonn, Y Yoshida, *et al.*, “Symmetry of charge order in cuprates,” *Nature materials* **14**, 796–800 (2015).
- [9] R Comin, A Frano, Michael Manchun Yee, Y Yoshida, H Eisaki, E Schierle, E Weschke, R Sutarto, F He, Anjan Soumyanarayanan, *et al.*, “Charge order driven by fermi-arc instability in  $Bi_2Sr_{2-x}La_xCuO_{6+\delta}$ ,” *Science* **343**, 390–392 (2014).
- [10] E Blackburn, J Chang, M Hücker, AT Holmes, Niels Bech Christensen, Ruixing Liang, DA Bonn, WN Hardy, U Rütt, Olof Gutowski, *et al.*, “X-ray diffraction observations of a charge-density-wave order in superconducting ortho-II  $YBa_2Cu_3O_{6.54}$  single crystals in zero magnetic field,” *Physical review letters* **110**, 137004 (2013).
- [11] MH Hamidian, SD Edkins, Sang Hyun Joo, A Kostin, H Eisaki, S Uchida, MJ Lawler, E-A Kim, AP Mackenzie, K Fujita, *et al.*, “Detection of a Cooper-pair density wave in  $Bi_2Sr_2CaCu_2O_{8+x}$ ,” *Nature* **532**, 343–347 (2016).
- [12] Wei Ruan, Xintong Li, Cheng Hu, Zhenqi Hao, Haiwei Li, Peng Cai, Xingjiang Zhou, Dung-Hai Lee, and Yayu Wang, “Visualization of the periodic modulation of Cooper pairing in a cuprate superconductor,” *Nature Physics* **14**, 1178–1182 (2018).

- [13] Matthias Vojta, Ying Zhang, and Subir Sachdev, “Competing orders and quantum criticality in doped antiferromagnets,” *Physical Review B* **62**, 6721 (2000).
- [14] Matthias Vojta, “Superconducting charge-ordered states in cuprates,” *Physical Review B* **66**, 104505 (2002).
- [15] Subir Sachdev and Rolando La Placa, “Bond order in two-dimensional metals with antiferromagnetic exchange interactions,” *Physical review letters* **111**, 027202 (2013).
- [16] Marcin Raczkowski, Manuela Capello, Didier Poilblanc, Raymond Frésard, and Andrzej M Oleś, “Unidirectional  $d$ -wave superconducting domains in the two-dimensional  $t$ - $j$  model,” *Physical Review B* **76**, 140505 (2007).
- [17] C Pépin, VS De Carvalho, T Kloss, and X Montiel, “Pseudogap, charge order, and pairing density wave at the hot spots in cuprate superconductors,” *Physical Review B* **90**, 195207 (2014).
- [18] Yuxuan Wang and Andrey Chubukov, “Charge-density-wave order with momentum  $(2\mathbf{Q}, 0)$  and  $(0, 2\mathbf{Q})$  within the spin-fermion model: Continuous and discrete symmetry breaking, preemptive composite order, and relation to pseudogap in hole-doped cuprates,” *Physical Review B* **90**, 035149 (2014).
- [19] WA Atkinson, Arno P Kampf, and S Bulut, “Charge order in the pseudogap phase of cuprate superconductors,” *New Journal of Physics* **17**, 013025 (2015).
- [20] Hanna Terletska, Tianran Chen, and Emanuel Gull, “Charge ordering and correlation effects in the extended Hubbard model,” *Physical Review B* **95**, 115149 (2017).
- [21] JPL Faye and D Sénéchal, “Interplay between  $d$ -wave superconductivity and a bond-density wave in the one-band hubbard model,” *Physical Review B* **95**, 115127 (2017).
- [22] AI Liechtenstein, Olle Gunnarsson, OK Andersen, and RM Martin, “Quasiparticle bands and superconductivity in bilayer cuprates,” *Physical Review B* **54**, 12505 (1996).
- [23] OK Andersen, AI Liechtenstein, O Jepsen, and F Paulsen, “LDA energy bands, low-energy hamiltonians,  $t'$ ,  $t''$ ,  $t_{\perp}(k)$ , and  $J_{\perp}$ ,” *Journal of Physics and Chemistry of Solids* **56**, 1573–1591 (1995).
- [24] Gabriel Kotliar, Sergej Y Savrasov, Gunnar Pálsson, and Giulio Biroli, “Cellular dynamical mean field approach to strongly correlated systems,” *Physical review letters* **87**, 186401 (2001).
- [25] SS Kancharla, B Kyung, David Sénéchal, M Civelli, Massimo Capone, G Kotliar, and A-MS Tremblay, “Anomalous superconductivity and its competition with antiferromagnetism in doped Mott insulators,” *Physical Review B* **77**, 184516 (2008).
- [26] David Sénéchal, “Bath optimization in the cellular dynamical mean field theory,” *Physical Review B* **81**, 235125 (2010).
- [27] David Sénéchal, “Cluster dynamical mean field theory,” in *Strongly Correlated Systems* (Springer, 2012) pp. 341–371.
- [28] Erik Koch, Giorgio Sangiovanni, and Olle Gunnarsson, “Sum rules and bath parametrization for quantum cluster theories,” *Physical Review B* **78**, 115102 (2008).
- [29] Alexandre Foley, Simon Verret, A-MS Tremblay, and David Senechal, “Coexistence of superconductivity and antiferromagnetism in the Hubbard model for cuprates,” *Physical Review B* **99**, 184510 (2019).
- [30] S Verret, J Roy, A Foley, M Charlebois, D Sénéchal, and A-MS Tremblay, “Intrinsic cluster-shaped density waves in cellular dynamical mean-field theory,” *Physical Review B* **100**, 224520 (2019).
- [31] Eduardo Fradkin, Steven A Kivelson, and John M Tranquada, “Colloquium: Theory of intertwined orders in high temperature superconductors,” *Reviews of Modern Physics* **87**, 457 (2015).
- [32] Erez Berg, Eduardo Fradkin, Steven A Kivelson, and John M Tranquada, “Striped superconductors: how spin, charge and superconducting orders intertwine in the cuprates,” *New Journal of Physics* **11**, 115004 (2009).
- [33] J-YP Delannoy, MJP Gingras, PCW Holdsworth, and A-MS Tremblay, “Néel order, ring exchange, and charge fluctuations in the half-filled hubbard model,” *Physical Review B* **72**, 115114 (2005).
- [34] Rinat Ofer, Galina Bazalitsky, Amit Kanigel, Amit Keren, Assa Auerbach, James S Lord, and Alex Amato, “Magnetic analog of the isotope effect in cuprates,” *Physical Review B* **74**, 220508 (2006).
- [35] Kristjan Haule and Gabriel Kotliar, “Strongly correlated superconductivity: A plaquette dynamical mean-field theory study,” *Physical Review B* **76**, 104509 (2007).